5th Australasian Congress on Applied Mechanics, ACAM 2007
10-12 December 2007, Brisbane, Australia

Limit Analysis of Strain Softening Frames Allowing for Geometric Nonlinearity

S. Tangaramvong[1] and F. Tin-Loi[1]

[1]School of Civil and Environmental Engineering, University of New South Wales, Sydney, Australia

Abstract: This paper extends classical limit analysis to account for strain softening and 2nd-order geometric nonlinearity simultaneously. The formulation is an instance of the challenging class of so-called (nonconvex) mathematical programs with equilibrium constraints (MPECs). A penalty algorithm is proposed to solve the MPEC. A practical frame example is provided to illustrate the approach.

Keywords: complementarity, geometry nonlinearity, holonomic analysis, limit analysis, strain softening.

1 Introduction

Classical limit analysis is a powerful and simple method for assessing the maximum load capacity of perfectly plastic structures, without the need to follow the whole time history of loading. However, the pair of dual bound theorems underpinning this classical approach is only strictly applicable to structures that satisfy some rather restrictive requirements, the main ones being perfect plasticity (e.g. no hardening or softening, normality and convexity of yield surface) and geometric linearity.

The present paper presents an extension of classical limit analysis to encompass a wider class of practical frame structures. In particular, both local softening and 2nd-order geometric nonlinearity are allowed for. The novel approach proposed still requires only a single step analysis, but, moreover, it can not only provide an upper bound to the maximum load but it will furnish the corresponding deformations as well.

The organization of this paper is as follows. In Section 2, the classical holonomic (path-independent) elastoplastic analysis formulation is reviewed. This forms the basis for formulating, in Section 3, the extended limit analysis problem as an MPEC. Section 4 then proposes an algorithm to solve the MPEC. The key idea is to reformulate the nonconvex MPEC as a standard nonlinear programming (NLP) problem using a penalty function. In Section 5, a realistic softening frame example is provided to illustrate application of the present approach and to highlight the influences of both softening and geometric nonlinearities. Finally, some conclusions are drawn in Section 6.

2 Holonomic Elastoplastic Analysis

It is first assumed, as is usual, that the structure has been discretized as an aggregate of finite elements. In the present case, the material behavior is conveniently established at an element level rather than at a material level, since the class of finite elements expressed in intrinsic, natural (in Prager's generalized sense) variables is adopted [1]. This implies that the scalar product of generalized stress and strain vectors represents virtual work in the element concerned and is invariant with respect to rigid body motion. Thus, for a generic self equilibrated 2-D frame element *i* in Figure 1, the generalized stress vector $\mathbf{s}^i \in \Re^3$ contains the three (independent) two end moments (s_2^i, s_3^i) and one axial force (s_1^i). The corresponding generalized strain vector $\mathbf{q}^i \in \Re^3$ then consists of the corresponding end rotations (q_2^i, q_3^i) and one axial deformation (q_1^i).

A simplified geometrically nonlinear approach, based on the well-known 2nd-order geometric theory [2], is adopted. It is thus assumed that displacements from the undeformed state are geometrically small [3]. For a generic frame element *i* (Figure 1), this 2nd-order geometric nonlinearity can be conveniently described by introducing an additional transverse force π_f^i as well as its corresponding displacement δ_f^i. Clearly, the force π_f^i and the displacement δ_f^i are sufficient to describe the configuration change of a member.

For elastoplastic members, material nonlinearity is included through the traditional concept of the plastic hinge model. More specifically, the formation of such hinges is confined only to member ends with the material between these ends assumed to be elasticity.

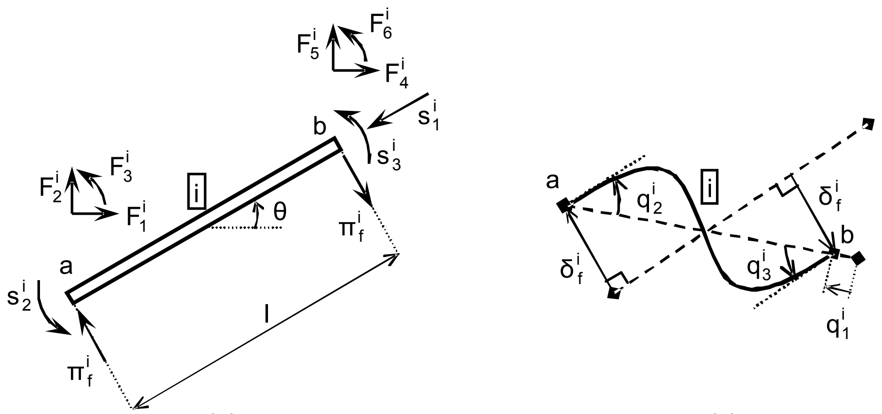

(a) (b)

Figure 1. Generic 2-D frame element *i* (a) stresses, (b) strains.

Holonomy, in the spirit of the deformation theory of plasticity, implies that elastic unloading from a plastic state does not occur and, hence, implies that any unloading from the active yield branch is reversible. For practical structures subjected to a monotonic loading regime, this assumption, as evidenced by recent work [4], leads to accurate predictions of actual structural responses. It is also assumed that associated elastoplasticity holds.

In terms of well-known notation and description [1], the governing holonomic formulation can now be written as follows:

$$\mathbf{C}_0^T\mathbf{s} + \mathbf{C}_f^T\boldsymbol{\pi}_f = \alpha\mathbf{f} + \mathbf{f}_d, \tag{1}$$

$$\mathbf{q} = \mathbf{C}_0\mathbf{u}, \tag{2}$$

$$\boldsymbol{\delta}_f = \mathbf{C}_f\mathbf{u}, \tag{3}$$

$$\mathbf{q} = \mathbf{e} + \mathbf{p}, \tag{4}$$

$$\mathbf{s} = (\mathbf{S}_0 + \mathbf{S}_g)\mathbf{e}, \tag{5}$$

$$\boldsymbol{\pi}_f = \mathbf{S}_f\boldsymbol{\delta}_f, \tag{6}$$

$$\mathbf{p} = \mathbf{N}\mathbf{z}, \tag{7}$$

$$\mathbf{w} = -\mathbf{N}^T\mathbf{s} + \mathbf{H}\mathbf{z} + \mathbf{r} \geq \mathbf{0},\ \mathbf{z} \geq \mathbf{0},\ \mathbf{w}^T\mathbf{z} = 0. \tag{8}$$

Vector and matrix quantities (indicated in bold) represent the unassembled contributions of corresponding elemental entities as concatenated vectors and block-diagonal matrices, respectively.

For a structure with *n* generic elements, *d* degrees of freedom, *m* natural generalized (stresses or strains) and *y* yield functions, (1) describes the equilibrium between nodal forces $\alpha\mathbf{f} + \mathbf{f}_d \in \Re^d$ (α is a scalar load multiplier, **f** is prescribed and $\mathbf{f}_d$ is fixed) and the stress components (namely natural stresses $\mathbf{s} \in \Re^m$ and additional auxiliary forces $p_f \in \Re^n$) through the linear compatibility matrix $\mathbf{C}_0 \in \Re^{m\times d}$ and the associated auxiliary compatibility matrix $\mathbf{C}_f \in \Re^{n\times d}$. Linear compatibility of strains $\mathbf{q} \in \Re^m$ with nodal displacements $\mathbf{u} \in \Re^d$ as in (2) then holds, provided that a linear relation between auxiliary displacements $d_f \in \Re^n$ and nodal displacements **u** is introduced as in (3).

The holonomic constitutive law is established in (4)-(8). In particular, the additivity of elastic $\mathbf{e} \in \Re^m$ and plastic $\mathbf{p} \in \Re^m$ strains is expressed by (4). The elastic constitution consists of two components, namely the relation between **s** and **e** in (5) as well as the relation between p_f and d_f in (6), where $\mathbf{S}_0 \in \Re^{m\times m}$ is the conventional linear stiffness matrix, $\mathbf{S}_g \in \Re^{m\times m}$ the geometric stiffness matrix and $\mathbf{S}_f \in \Re^{n\times n}$ the auxiliary stiffness matrix. Plastic strains **p** are defined by an associated flow rule in (7) through matrix $\mathbf{N} \in \Re^{m\times y}$ (outward normals to yield surface) and plastic multipliers $\mathbf{z} \in \Re^y$. A piecewise linear yield function vector $\mathbf{w} \in \Re^y$ accommodates, through $\mathbf{H} \in \Re^{y' y}$, a wide class of hardening [1] or softening [4] laws. Yield limits are defined by vector $\mathbf{r} \in \Re^y$. Finally, a complementarity relationship in (8), between the sign-constrained total quantities **w** and **z**, allows for the reversibility of plastic multipliers **z**.

To clarify the assumed 2nd-order geometry approach, consider again generic frame element i in Figure 1. From this figure, it is straightforward to obtain specific expressions of some key vectors and matrices, used in (1), (3), (5) and (6) for each element i, as follows:

$$\mathbf{C}_f^i = [-\sin\theta \quad \cos\theta \quad 0 \quad \sin\theta \quad -\cos\theta \quad 0], \mathbf{S}_g^i = \left(\frac{-s_1^i}{l}\right)\begin{bmatrix} 0 & 0 & 0 \\ 0 & 2l^2/15 & -l^2/30 \\ 0 & -l^2/30 & 2l^2/15 \end{bmatrix}, S_f^i = \left(\frac{-s_1^i}{l}\right)\Bigg\} \tag{9}$$

Clearly, these quantities are written solely in terms of an unknown variable s_1^i. The geometrically linear case is simply recovered by eliminating all nonlinear terms (e.g. $\mathbf{S}_g = \mathbf{0}$ and $\mathbf{S}_f = \mathbf{0}$).

When such members as heavily loaded columns are simultaneously subject to significant axial and flexural forces, the effects of axial forces must be included in the softening yield condition. Without undue loss of generality, the following hexagonal yield locus for the “start” hinge “*a*” of an element i, typical of an I-steel section under combined bending and axial forces, is adopted.

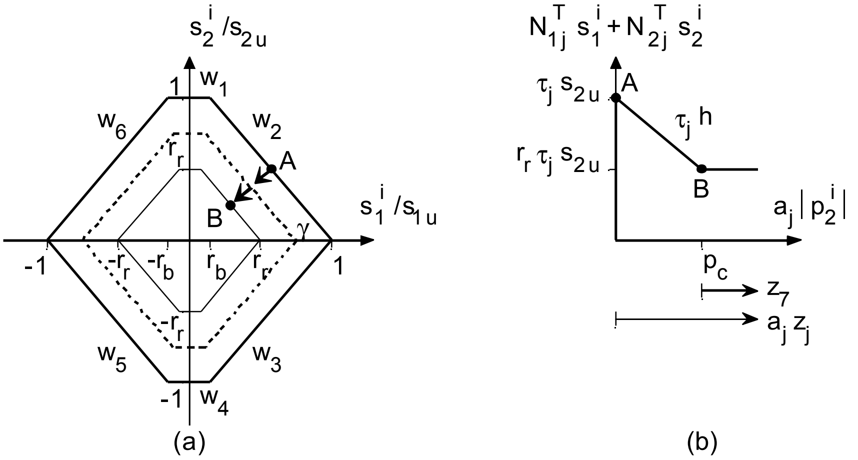

Figure 2. Softening law (a) interaction between s_1^i and s_2^i (b) softening behavior of yield plane j.

Positive and negative flexural/axial properties are assumed to be identical, with a reduction of the pure bending capacity occurring when the axial force reaches a fraction r_b (normally set to 0.15) of the pure axial capacity. The yield functions (8) for this isotropic softening model are described as follows [4]:

$$\left.\begin{array}{l} \mathbf{w}^{aT} = [w_1 \quad w_2 \quad w_3 \quad w_4 \quad w_5 \quad w_6 \quad w_7], \mathbf{s}^{aT} = [s_1^i \quad s_2^i], \mathbf{z}^{aT} = [z_1 \quad z_2 \quad z_3 \quad z_4 \quad z_5 \quad z_6 \quad z_7], \\ \mathbf{N}^{aT} = \begin{bmatrix} 0 & 1 \\ \tilde{n}\tan\gamma & 1 \\ \tilde{n}\tan\gamma & -1 \\ 0 & -1 \\ -\tilde{n}\tan\gamma & -1 \\ -\tilde{n}\tan\gamma & 1 \\ 0 & 0 \end{bmatrix}, \mathbf{H}^a = h\begin{bmatrix} a_1 & a_2 & a_3 & a_4 & a_5 & a_6 & -1 \\ \tau a_1 & \tau a_2 & \tau a_3 & \tau a_4 & \tau a_5 & \tau a_6 & -\tau \\ \tau a_1 & \tau a_2 & \tau a_3 & \tau a_4 & \tau a_5 & \tau a_6 & -\tau \\ a_1 & a_2 & a_3 & a_4 & a_5 & a_6 & -1 \\ \tau a_1 & \tau a_2 & \tau a_3 & \tau a_4 & \tau a_5 & \tau a_6 & -\tau \\ \tau a_1 & \tau a_2 & \tau a_3 & \tau a_4 & \tau a_5 & \tau a_6 & -\tau \\ \frac{a_1}{s_{2u}} & \frac{a_2}{s_{2u}} & \frac{a_3}{s_{2u}} & \frac{a_4}{s_{2u}} & \frac{a_5}{s_{2u}} & \frac{a_6}{s_{2u}} & \frac{-1}{s_{2u}} \end{bmatrix}, \mathbf{r}^a = \begin{bmatrix} s_{2u} \\ \tau s_{2u} \\ \tau s_{2u} \\ s_{2u} \\ \tau s_{2u} \\ \tau s_{2u} \\ 1-r_r \end{bmatrix}, \end{array}\right\} \tag{10}$$

where $\tilde{n} = s_{2u}/s_{1u}$; $h = -s_{2u}(1-r_r)/p_c$; $\tau = 1 + r_b \tan\gamma$; $a_j = p_c/|p_{cj}|$ for all $j \in \{1,\ldots,6\}$; t_j (j = 1,4) = 1 and t_j (j = 2,3,5,6) = t; s_{1u} and s_{2u} are respectively axial and flexural yield capacities; r_r is the residual stress state; p_c (e.g. $p_c = p_{c1}$) is a single arbitrarily assumed critical plastic strain while p_{cj} (j = 1,…,6) are the actual critical plastic strain values.

Relation set (1)-(8) is a mixed complementarity problem (MCP). This holonomic analysis is carried out by using an existing nonholonomic code [4], albeit modified to allow all plastic multipliers to decrease in a reversible fashion. For the 2nd-order geometry case, an iterative scheme, in view of nonlinear terms present (namely $\mathbf{S}_g$ in (5) and $\mathbf{S}_f$ in (6)), is required; nonlinear quantities are linearized at each iteration by using previously found solutions as data. The holonomic implementation uses the MCP solver PATH [5] within the GAMS/MATLAB mathematical programming modeling environment; where GAMS is an acronym for General Algebraic Modeling System [6].

3 Extended Limit Analysis Problem as an MPEC

Our proposed extended limit analysis is conceptually simple in that it aims to maximize the load factor (assumed to be a variable) under the same relation set (1)-(8) that would apply to a holonomic analysis under load control. Thus, this can be cast as the following optimization problem in variables $(\alpha, \mathbf{s}, \boldsymbol{\pi}_f, \mathbf{u}, \mathbf{z})$:

$$\left.\begin{aligned}
&\text{Maximize} && \alpha \\
&\text{subject to} && \mathbf{C}_0^T\mathbf{s} + \mathbf{C}_f^T\boldsymbol{\pi}_f - \alpha\mathbf{f} - \mathbf{f}_d = \mathbf{0}, \\
& && \left(\mathbf{S}_0 + \mathbf{S}_g\right)^{-1}\mathbf{s} - \mathbf{C}_0\mathbf{u} + \mathbf{N}\mathbf{z} = \mathbf{0}, \\
& && \mathbf{S}_f^{-1}\boldsymbol{\pi}_f - \mathbf{C}_f\mathbf{u} = \mathbf{0}, \\
& && \mathbf{w} = -\mathbf{N}^T\mathbf{s} + \mathbf{H}\mathbf{z} + \mathbf{r} \geq \mathbf{0}, \mathbf{z} \geq \mathbf{0}, \mathbf{w}^T\mathbf{z} = 0.
\end{aligned}\right\} \tag{11}$$

Optimization problem (11) is an MPEC [7], for which the equilibrium constraints are complementarity constraints. Problems of this type cannot yet be solved with certainty. There are various reasons why this is so. In the first instance, as is well-known from the integer programming literature, disjunctive constraints such as complementarity conditions in (11) are very difficult to handle. It is often stated that such constraints constitute a combinatorial "curse" for MPECs. Moreover, the feasible region of an MPEC, with its lack of convexity, smoothness and sometimes even connectivity, often leads to severe numerical instability in any algorithm. In spite of the various numerical difficulties, the authors have had considerable success in solving similar MPECs (e.g. [8]). The general strategy adopted is to reformulate MPEC (11) as a standard NLP problem by suitably "treating" the complementarity conditions.

As discussed earlier for the holonomic analysis case, an iterative scheme is still required to solve (11) since the two matrices $\mathbf{S}_g$ and $\mathbf{S}_f$ involve unknown stresses $\mathbf{s}$. Our algorithm therefore involves a series of iterative MPEC solves as follows:

1. At $i = 0$, initialize $\mathbf{s}_i = \mathbf{0}$.
2. Set $i = i + 1$. Assume that $\mathbf{s}_i = \mathbf{s}_{i-1}$, and calculate new $\mathbf{S}_g$ and $\mathbf{S}_f$. Then, formulate and solve MPEC (11). Obtain the new estimates for α_i, $\mathbf{s}_i$, $p_{f,i}$, $\mathbf{u}_i$ and $\mathbf{z}_i$.
3. Check convergence: if max(abs($\mathbf{s}_i - \mathbf{s}_{i-1}$)) $\leq 10^{-6}$, then terminate. Else, repeat Step (2).

4 Penalty Algorithm to Solve the MPEC

The penalty algorithm is well-known in the mathematical programming literature [7]. This has also been successfully used in various mechanical problems involving MPECs, e.g. in a frictional contact problem [8]. The basic idea is to transfer the complementarity term to the objective function and penalize it. In particular, this involves adding the term $-\mu\mathbf{w}^T\mathbf{z}$ to the objective function, where μ is a penalty parameter. As a result, MPEC (11) is converted to the following NLP problem:

$$\left.\begin{aligned}
&\text{Maximize} && \alpha - \mu\mathbf{w}^T\mathbf{z} \\
&\text{subject to} && \mathbf{C}_0^T\mathbf{s} + \mathbf{C}_f^T\boldsymbol{\pi}_f - \alpha\mathbf{f} - \mathbf{f}_d = \mathbf{0}, \\
& && \left(\mathbf{S}_0 + \mathbf{S}_g\right)^{-1}\mathbf{s} - \mathbf{C}_0\mathbf{u} + \mathbf{N}\mathbf{z} = \mathbf{0}, \\
& && \mathbf{S}_f^{-1}\boldsymbol{\pi}_f - \mathbf{C}_f\mathbf{u} = \mathbf{0}, \\
& && \mathbf{w} = -\mathbf{N}^T\mathbf{s} + \mathbf{H}\mathbf{z} + \mathbf{r} \geq \mathbf{0}, \mathbf{z} \geq \mathbf{0}.
\end{aligned}\right\} \tag{12}$$

A negative penalization is necessary in view of a maximization requirement. Clearly, with increasing values of μ, the complementarity term is driven towards zero. The algorithm simply increases the penalty parameter m at each NLP iterate, each represented by (12), until a preset complementarity tolerance (e.g. $\mathbf{w}^T\mathbf{z} \le 10^{-6}$) has been reached. The attraction of this method is that each penalty subproblem is a standard NLP problem that can be solved by any one of readily available and powerful NLP codes, such as CONOPT [9].

Typical starting values for m are within the range 0.1-1, with an update of m = 10m after each NLP solve. A good specification of initial variables (e.g. $\mathbf{w} = \mathbf{r}$) often helps the NLP solves.

5 Illustrative Example

The realistic nine storey portal frame, as shown in Figure 3a, is considered. It is subjected to increasing vertical point loads of 6α (kN) and increasing lateral loads (kN) governed by load factor α; v denotes the corresponding top storey sway displacement (m). The structure was discretized into 126 elements, 93 nodes, 261 degrees of freedom and 213 critical sections (namely at columns ends, beam ends and mid-span).

Three holonomic analysis cases were carried out: Case a (perfectly plastic, combined stresses and small deformation), Case b (softening, combined stresses and small deformation), and Case c (softening, combined stresses and 2nd-order geometry). This was the followed by a corresponding series of extended limit analyses that aimed to capture the maximum load in each of the three indicated cases.

Steel sections with $E = 2\times10^8$ kNm^{-2} were adopted: 400WC328 for all columns (s_{2u} = 1988 kNm, s_{1u} = 11704 kN) and 460UB82.1 for all beams (s_{2u} = 552 kNm, s_{1u} = 3150 kN). For the softening Cases b and c (in Figure 2 with r_r = 0.7, r_b = 0.15, tang = 1/0.85 and a_j = 1 for all j), the parameters employed were: for columns h = –18418.78 kNm; for beams h = –4852.04 kNm at beam ends, h = –2426.02 kNm at mid-span.

The overall holonomic α-v responses for Cases a to c are depicted in Figure 3b. Also shown (as •) are the results of the extended limit analyses. In particular, the maximum loads computed were: α = 91.754 with v = 0.75 m for Case a, α = 79.709 with v = 0.330 m for Case b, and α = 69.616 with v = 0.287 m for Case c.

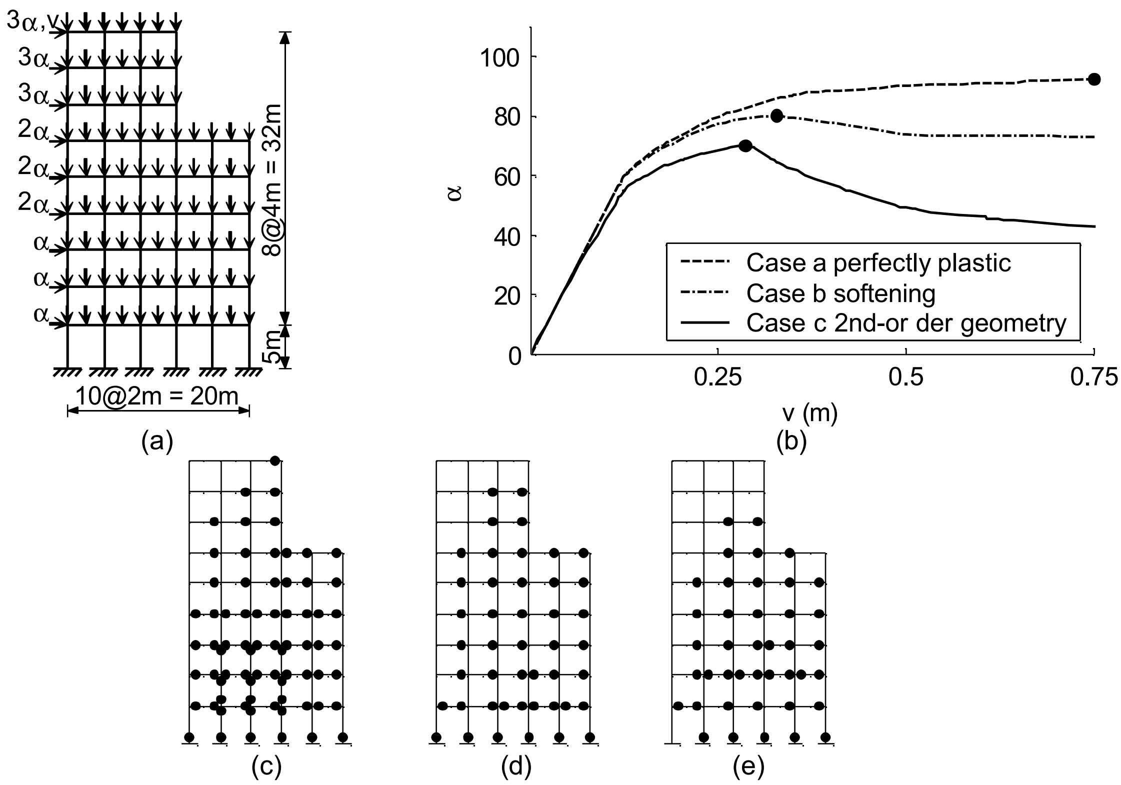

Figure 3. Frame example (a) nine storey portal frame, (b) holonomic α-v responses, (c)-(e) hinge dispositions at peak loads for Cases a to c, respectively (• denotes hinge on softening branch).

As is clearly evident, the accuracy of these results can be confirmed through comparison with the actual holonomic step-by-step responses. Hinge dispositions at peak loads of all Cases a to c are shown respectively in Figures 3c-3e. In all runs, the penalty algorithm had no difficulty in providing the limit loads. For the 2nd-order geometry Case c, the total 17 MPEC iterates were required to converge to the solution. Some details of hinge activations are provided in the following.

The holonomic analyses for Cases a and b indicated that the first and second hinges formed at some beam sections when α = 55.359 and 55.374, respectively. In Case a, a column section started to yield at α = 69.981, and the analysis was terminated at α = 91.754 with v = 0.75 m. In Case b, the first (column) hinge formed at α = 69.351, and the maximum load was attained at α = 79.709, approximately 15% less than that of the perfectly plastic Case a. In the 2nd-order geometry Case c, the overall load behavior indicated a weaker structure than that of the small deformation Case b. Not only was a smaller maximum load attained for Case c, but the post peak behavior also showed a sharper drop. Beams and columns initiated their first hinge at α = 51.949 and 65.167, respectively. The maximum load was reached at α = 69.616, some 15% less than that of Case b. These load reductions, of course, indicate the importance of accounting for both softening and geometric nonlinearity.

6 Conclusions

A novel approach for extending classical limit analysis for a wide class of the elastoplastic structures has been presented. The analysis can account for local softening behavior and 2nd-order geometric nonlinearity. For the frames considered, the yield condition is governed by combined flexural and axial forces. At variance with a classical limit analysis, the proposed approach is able to provide simultaneously the maximum load and corresponding deformations in a single step.

The formulation takes the form as a nonconvex optimization problem referred to as an MPEC. In spite of the underlying well-known difficulties in solving such problems, a penalty NLP-based algorithm has been successfully used to solve our MPEC. The efficiency and robustness of the approach has been tested using a large number of examples, one of which is presented in this paper.

The particular example given concerns a realistic steel frame example. The results highlight the fact that it is important to consider the effects of both softening (under combined stresses) and geometric nonlinearity in the correct estimation of the maximum load capacity of such structures. Ignoring any of these effects can lead to unsafe load predictions.

Acknowledgement

This research was supported by Australian Research Council, ARC Discovery Grant DP044979.

References

[1] G. Maier, 'A matrix theory of piecewise linear elastoplasticity with interacting yield planes', *Meccanica*, **5**, 54-66, 1970.

[2] J.S. Przemieniecki, *Theory of Matrix Structural Analysis*, Dover Publication Inc, New York, 1985.

[3] D. Lloyd Smith, 'Large-displacement elastic-plastic analysis of frames', in *Engineering Plasticity by Mathematical Programming*, M.Z. Cohn and G. Maier (editors), Pergamon, New York, 1979, Chapter 20.

[4] S. Tangaramvong and F. Tin-Loi, 'A complementarity approach for elastoplastic analysis of strain softening frames under combined bending and axial force', *Engineering Structures*, **29**, 742-753, 2007.

[5] S.P. Dirkse and M.C. Ferris, 'The PATH solver: a nonmonotone stabilization scheme for mixed complementarity problems', *Optimization Methods and Software*, **5**, 123-156, 1995.

[6] A. Brooke, D. Kendrick, A. Meeraus and R. Raman, *GAMS: A User's Guide*, GAMS Development Corporation, Washington, DC20007, 1998.

[7] Z.Q. Luo, J.S. Pang and D. Ralph, *Mathematical Programs with Equilibrium Constraints*, Cambridge University Press, Cambridge, 1996.

[8] F. Tin-Loi, S. Tangaramvong and S.H. Xia, 'Limit analysis of frames involving unilateral supports with frictional contact', *International Journal of Mechanical Sciences*, **49**, 454-465, 2007.

[9] A. Drud, 'CONOPT – a large-scale GRG code', *ORSA Journal of Computing*, **6**, 207-216, 1994.